RF Heating of Implanted Spinal Fusion Stimulator During Magnetic Resonance Imaging

Chung-Kwang Chou,* *Fellow, IEEE*, John A. McDougall, *Member, IEEE*, and Kwok W. Chan, *Member, IEEE*

***Abstract*—Radio frequency (RF) heating of an implanted spinal fusion stimulator (SpF) during magnetic resonance imaging (MRI) was studied on a full-size human phantom. Heating during MRI scans (GE Signa 4X, 1.5 T) was measured with RF-transparent fiberoptic sensors. With the implant correctly connected, the maximum temperature rises were less than 2 °C during the 26 min that the scans were at maximum RF power. At the tip of a broken stimulator lead (connecting the SpF generator and its electrodes), the maximum temperature rise was 11–14 °C. Regular 4-min scans of the spinal cord produced similar temperature rises at the broken tip. After the generator and the leads were removed, heating at the electrode connector tip was less than 1.5 °C. The control temperature rises at the same locations, without the stimulator, were less than 0.5 °C. This study shows that spinal fusion stimulator heating is within the Food and Drug Administration safety guideline of 2 °C. However, if a lead wire is broken, it is unsafe during MRI scans. Radiological examinations will be necessary to ensure the integrity of the implant.**

***Index Terms*—Bone fusion, induced current, phantom model, RF energy absorption, thermal effect.**

I. Introduction

THE spinal fusion stimulator (SpF), (Electro-Biology, Inc., Parsippany, NJ 07054-1079) has been used to increase bone fusion in about 50 000 patients. The stimulator consists of a small direct-current generator encased in a titanium shell that acts as an anode. Two insulated nonmagnetic silver/stainless steel leads provide a connection to two titanium electrodes which serve as the cathodes (Fig. 1). A continuous 20-μA current is produced. The cathodes are embedded in pieces of bone grafted on the lateral aspects of the fusion sites. There are potential health effects when a patient wearing the SpF requires diagnostic magnetic resonance imaging (MRI). In a strong static magnetic field and a pulsed radio-frequency (RF) field, five potential adverse effects are anticipated with metallic implants: 1) force on the implant by the strong static magnetic field; 2) current in the SpF, induced by the RF field; 3) damage of the SpF circuitry by pulsed RF exposure; 4) heating of the SpF and adjacent tissue due to RF energy absorption; and 5) MRI image distortion caused by the SpF. In this study, only the RF heating will be addressed. The present Food and Drug Administration's recommended limits of RF heating during MRI scanning are 1 °C in the brain, 2 °C in the torso, and 3 °C in the extremities [1].

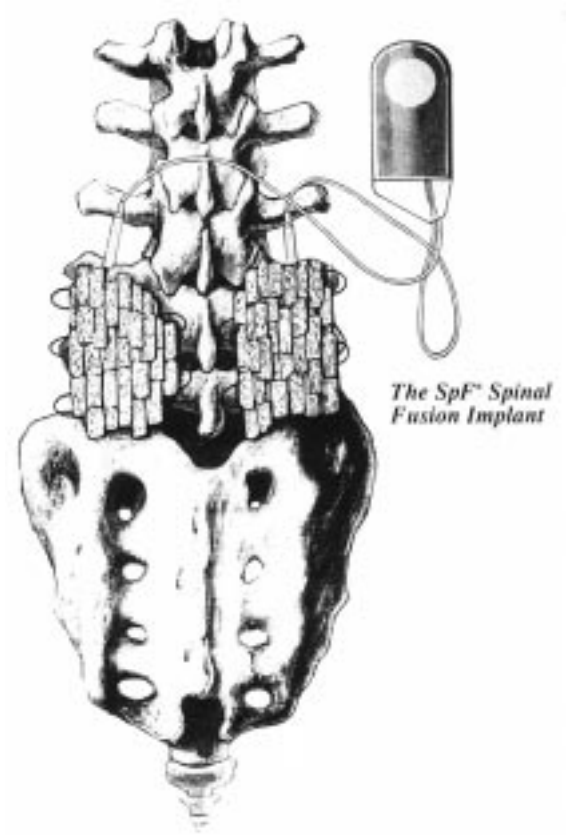

Fig. 1. Schematic of spinal fusion stimulator (SpF) showing electrodes at L4-L5 level and under bone chips.

Since RF energy absorption is a function of body size, the heating of the SpF can only be tested in a full-size phantom human model. Because the RF field is strongest inside the MRI scanner, the effect of the head and lower legs on the energy absorption in the lower back should be minimal; however, since no confirmable data were available, a whole-body model was used. The determination of implant heating in an RF field is similar to the measurement of specific absorption rate (SAR). The difference is due to the low RF power and long duration used during an MRI procedure. For SAR determination, high power and short duration are necessary to minimize thermal diffusion [2]. The tissue temperature during long RF exposures finally reaches a steady state when heat loss (due to thermal diffusion) equals power dissipation. In this study, temperature rises adjacent to the implant during

Manuscript received June 28, 1996; revised January 24, 1997. This work was supported by Electro-Biology Inc., Parsippany, NJ. *Asterisk indicates corresponding author*.

*C. K. Chou is with the Department of Radiation Research, City of Hope National Medical Center, 1500 East Duarte Road, Duarte, CA 91010-3000 USA (e-mail: ckc@smtplink.coh.org).

J. A. McDougall and K. W. Chan are with the Department of Radiation Research, City of Hope National Medical Center, Duarte, CA 91010-3000 USA.

Publisher Item Identifier S 0018-9294(97)02955-8.

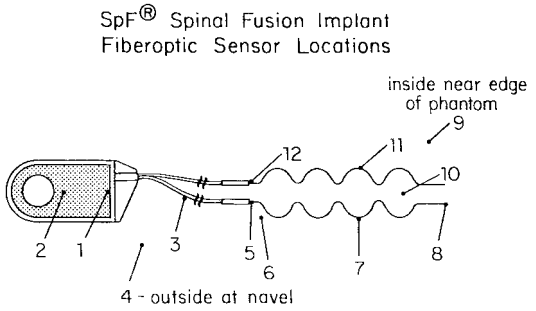

Fig. 2. Locations of fiberoptic sensors for intact implant: 1) edge of generator, 2) center of generator surface, 3) lead wire, 4) navel, 5) beginning of electrode, 6) in tissue near location 5, 7) middle of electrode, 8) tip of electrode, 9) in tissue near edge of right waist, 10) in tissue between electrodes, 11) middle of electrode, and 12) beginning of electrode.

MRI exposures were measured. Because blood flow was not simulated in the static phantom, the temperatures in the phantom around the SpF would be a worst case scenario. A similar study on auditory implants has been reported [3].

II. Methods

To characterize heating of SpF during MRI, experimental techniques included phantom construction and temperature measurement using RF transparent fiberoptic probes.

A. Phantom Model

A 1.6-m-tall fiberglass-shell human model was constructed [4]. The model was bisected frontally. Flanges at the cut edge were held by nylon screws. The model had phantom brain, muscle, lungs, and bone. The phantom skull was filled with phantom brain and the chest with phantom lungs; the remaining space between the skeleton and fiberglass shell was filled with phantom muscle. The phantom head was removable at the neck. An oval window (14×21 cm) on the back of the fiberglass model was opened for implant modification. Catheter tubings made of thin wall AWG 22 Teflon were positioned at nine locations on the electrodes and generator shell. Fig. 2 shows the locations of the nine catheters on the implant. These catheters were used to position the temperature sensors at the end of the catheters. The window was covered with a fiberglass plate tightened with nylon screws.

The phantom bone was made according to the formula of Hartsgrove *et al.* [5] and was a mixture of 36% two-ton epoxy, 36% hardener (Devcon), and 28% 2 M KCl. The materials, enough to make an entire skeleton, were sent to Medical Plastic Laboratories (Gatesville, TX) who specializes in making plastic skeletons for teaching. The skeleton was kept in a moisture-tight plastic bag and periodically soaked in 2 M KCl solution. The dielectric constant of the bone material is 14, and its conductivity is 0.8 S/m at 100 MHz. The dielectric properties at the MRI RF frequency of 63.8 MHz should be close to that at 100 MHz. The disks between the vertebrae were made of PVC with a dielectric constant of 2.8. New mixes were developed to simulate brain and muscle at 64 MHz [3]. The brain was mixed with 93% H_2O, and 7% TX-151 (a gelling agent), the muscle with 91.48% H_2O, 8.4% TX-151 and 0.12% NaCl. At 20 °C room temperature, the phase shift and attenuation of the mixtures inside a coaxial slotted line were measured with a network analyzer, as described by Chou *et al.* [6]. Dielectric constant and conductivity were calculated from the measurements. The dielectric constant and conductivity of the phantom brain and muscle were 78.12 and 0.52 S/m, and 79.8 and 0.8 S/m, respectively. These dielectric properties are well within the range of published data [7]. For the lung, a mixture of 47% phantom muscle and 53% polyethylene powder, following Hartsgrove *et al.* [5], was used.

Four conditions were simulated: 1) Intact implant: The SpF (model 2T) was implanted as in a patient, according to the instructions of B. Simon from Electro-Biology Inc. Location of temperature sensors are shown in Fig. 2. 2) One wire broken: Same as Condition 1 except the left lead in the body from the generator to the electrode was cut at the middle section. A 1-mm wire was exposed. Two catheters were attached to the ends of the broken lead. Sensor #1 (all sensors were inserted in blind-end AWG22 Teflon tubings) was relocated to the end of the broken wire connected to the generator. Sensor #3 was attached to the end of the broken wire connected to the electrode. 3) Titanium generator removed: The generator shell and leads were removed, and the two electrodes remained. Sensors #1 and #3 were attached to the tips of the right and left electrode pins. In patients, six months after implant, the generator and leads are removed surgically. Most implant patients stay in this condition. 4) No implant: The remaining electrodes were removed. All temperature sensors remained at the same locations as in Condition 1 but without the implant. This was the control case.

B. MRI Exposure

According to the manufacturer (General Electric) a maximum RF heating condition on a GE Signa 4X, 1.5 T MRI unit could be obtained by setting the following parameters: scan plane, axial; pulse sequence, spin-echo; echo time, 25 ms; repetition time, 134 ms; field of view, 48 cm; slice thickness, 20 mm; matrix, 128; direction of slice acquisition, anterior to posterior; number of excitation, 94; number of slices, one; number of echos, four; phasing, anterior to posterior; transmitter gain, 200; and scan time, 26 min. Maximum switched magnetic gradient was 16.7 T/m/s. The console-predicted whole-body averaged SAR for these settings and a body weight of 150 lb was 1.095 W/kg, using the body coil. Eight worst case MRI RF heating tests were conducted for the four implant conditions. For every condition, two consecutive scans were done to assure repeatability.

For Condition 2, two additional regular MRI setting scans, as used on patients, were taken to compare with the worst case RF heating. The settings were as follows for basic spin echo: scan plane, axial; pulse sequence, spin-echo; echo time, 17 ms; repetition time, 650 ms; field of view, 14 cm; slice thickness, 5 mm; matrix, 192; direction of slice acquisition, anterior-posterior; number of excitation, two; number of slices, one; number of echos, one; phasing, anterior-posterior; transmitter gain, 200; and scan time, 4 min and 18 s. The whole-body averaged SAR for these settings was 0.914 W/kg.

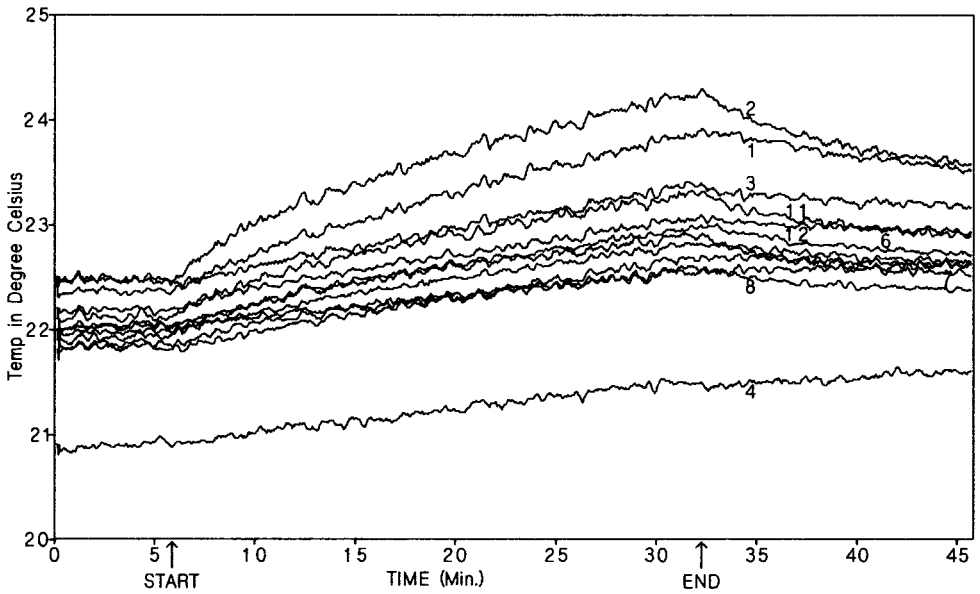

Fig. 3. Temperature data of an intact SpF implant in a phantom model during a worst case MRI scan. The highest temperature was recorded at the center of the generator. The second highest was at the edge of the generator.

C. Temperature Measurements

Luxtron (Santa Clara, CA) Model 3000 fiberoptic sensors [8] were used to map temperature distribution at the electrodes and generator. Twelve sensors were inserted into preimplanted catheters to record the temperatures in a notebook computer. Nine sensors were used to monitor the temperatures adjacent to the stimulator. Sensor #4 was attached near the navel for room air temperature monitoring. Sensor #9 was in the right side of the waist (2.5-cm deep from surface) and Sensor #10 was between the electrodes to measure tissue heating (Fig. 2). The night before the test, the model, the Luxtron fiberoptic temperature measurement instrument, and the computer were set up in the MRI and the control rooms. MRI heating tests were conducted on two consecutive weekends. At the beginning of the test, B. Simon of Electrobiology, Inc. showed the proper placement of the SpF. All pilot runs were done on the first weekend to debug the procedure. During the second weekend, the measurements were repeated.

III. Results

Condition 1: Fig. 3 shows the temperature results in the model with an intact implant. The highest temperature rise was at the center of the titanium generator surface (from 22.5 to 24.3 °C), and the second highest was at the edge of the generator (from 22.5 to 24 °C). Note, the room temperature rise was 0.5 °C. Therefore, with implanted SpF the maximum temperature rise was less than 2 °C measured at the center of the generator surface. The temperature rises at the electrodes were less than 1 °C. There temperature changes at the tip of the electrode (Sensor #8) were smaller than other locations.

Condition 2: When one of the generator leads was broken at the middle section, the temperature rise was as high as 11 °C (from 23 °C to 34 °C), as shown in Fig. 4. This occurred at Sensor #1, which was connected to the end of the broken lead connected to the generator. The other end of the broken lead (Sensor #3) had only 3 °C rise (23 °C to 26 °C). The initial peaks shown in Fig. 4 were due to RF heating during MRI tuning. Although the temperature of Sensor #2 (generator center) remained high, Sensor #11 (at the center of the electrode of the uncut side) was the third highest in temperature rise. In a repeated run (data not shown), the highest temperature rise was about 14 °C. When a regular spinal examination was scanned for 4 min, the maximum increase was also about 12 °C (Fig. 5).

Condition 3: Measurements made after the generator and the associated leads were removed from the phantom showed a maximum temperature rise of about 1.5 °C at one of the electrode pins (Sensor #1 in Fig. 6). Taking the room temperature rise (Sensor #4) into consideration, all other sensors showed insignificant temperature changes.

Condition 4: Finally, the temperature rises at the same locations without the implant were less than 0.5 °C (Fig. 7). The highest rise was at Sensor #9 which was at the waist where maximum tissue heating is expected.

IV. Discussion

Shellock *et al.* [9] monitored body and skin temperatures of 25 patients before and immediately after MRI of the spine. The average temperature rise at the isocenter position was 0.8 °C. Davis *et al.* [10] showed that in cylindrical saline agar phantoms the temperature increased more at the periphery than near the center. This is consistent with the RF induced eddy-current heating, which is size dependent. In our previous study [3], we were unable to detect heating in a head model but measured a temperature rise of 2 °C at the arm when the chest region was at the center of the field. The size of the object determines the energy coupling. In this study, Sensor #9 was placed at the edge of the waist to monitor the maximum RF heating of the phantom tissue. The heating was less than 0.5 °C. Davis *et al.* [10] also pointed out that hot spots can form in inhomogeneous tissues. Energy absorption, and therefore temperature rise, is a complicated

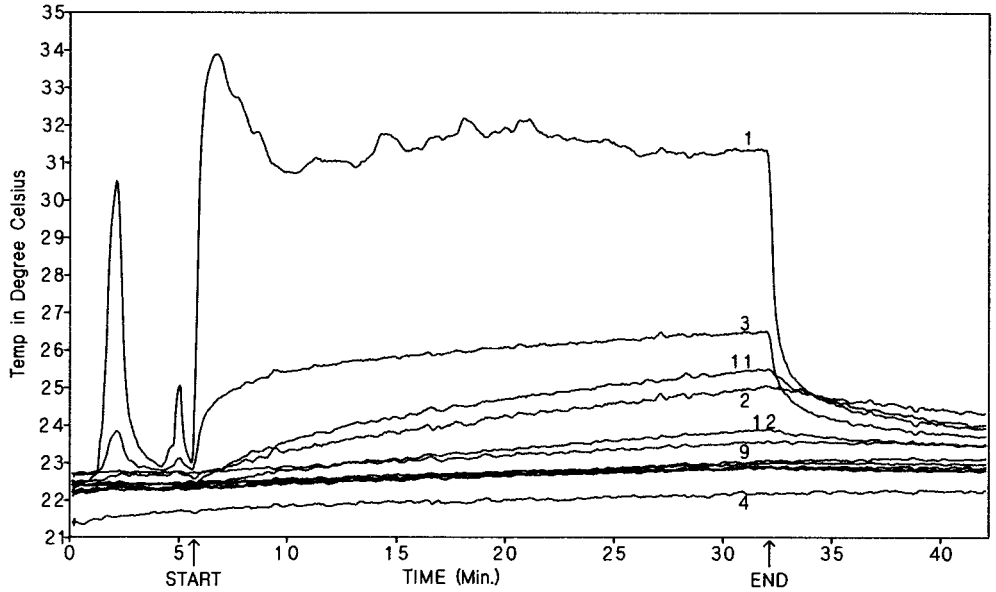

Fig. 4. Temperature data of SpF implant in a phantom model with a broken lead during a worst case MRI scan (Run #1). A rise of 11 °C was observed at the tip of the broken lead connected to the generator. The initial peaks were due to RF heating during MRI tuning.

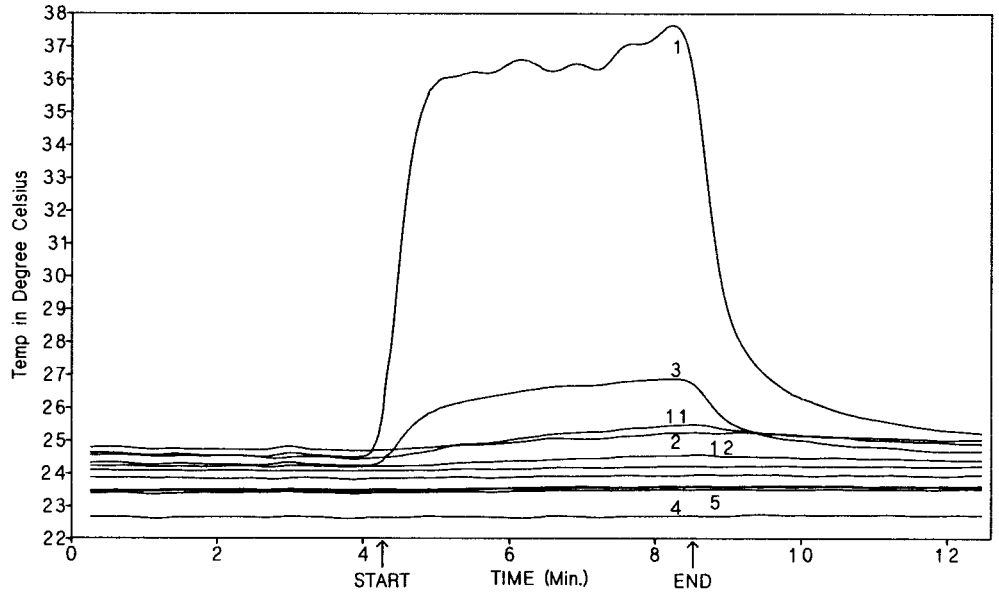

Fig. 5. Temperature data of SpF implant in a phantom model with a broken lead during a regular 4-min MRI scan. A rise of 12 °C was observed at the tip of the broken lead connected to the generator.

function of many variables such as dielectric properties, model size, model shape, orientations, and frequency [2]. Results in this study indicate that the physical condition of an implant also influences the temperature distribution.

Concerning heating of metallic implants during MRI, Buchli *et al.* [11] could not detect temperature changes in a large aluminum sheet, a hip joint prosthesis, and an osteosynthetic plate. Zhang *et al.* [12] measured temperature rises on insulated nickel–chromium electrodes placed between saline bags. They found no significant temperature increase in their experiments. Their electrodes were not in electrical contact with the saline and no temperature at the tip of the electrodes was measured. Fagan *et al.* [13] and Shellock *et al.* [14], [15] have shown that breast tissue expanders, a vascular access port, and a heart valve induced 0.3 °C or less temperature rise in *ex vivo* testings and have concluded that it is safe to apply MRI to patients with these implants. In our study, we used a model with its size, shape, and dielectric properties as close to those of a human as possible. This model did not include blood flow and therefore simulated a worst case scenario.

The question whether the eddy-current heating due to the switched gradient field could contribute to the observed heating. Shellock and Kanal [16] indicated that thermal effects that result from the gradient switching during MRI are negligible. In a future experiment, this can be tested by turning on only the switched gradient and not the RF fields.

The National Council on Radiation Protection and Measurements [17] in its Report 67 Appendix G on "Calculation of

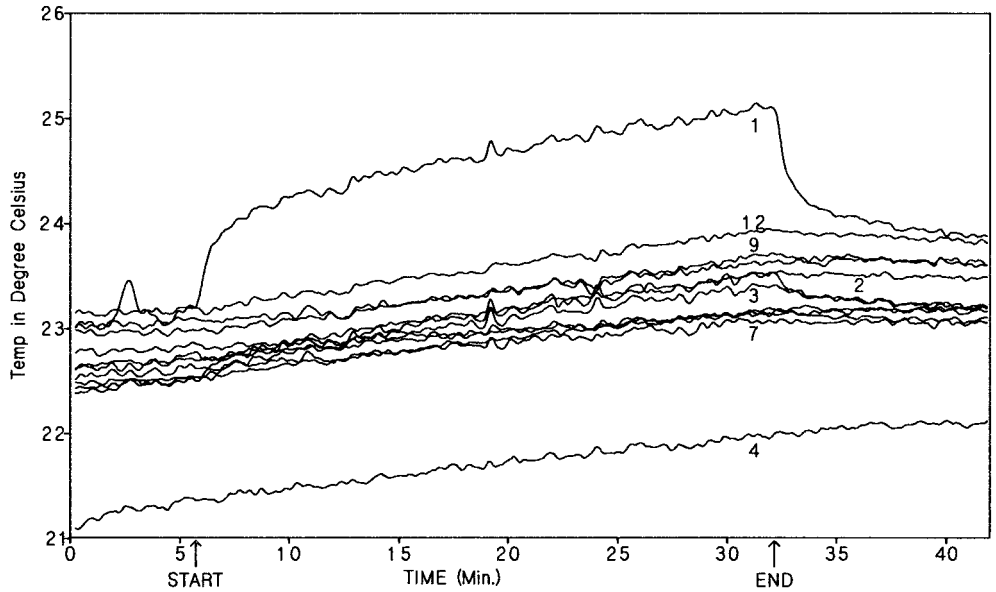

Fig. 6. Temperature data of SpF implant electrodes only in a phantom model during a worst case MRI scan. A rise of 1.5 °C was observed at the tip of the electrode insertion pin.

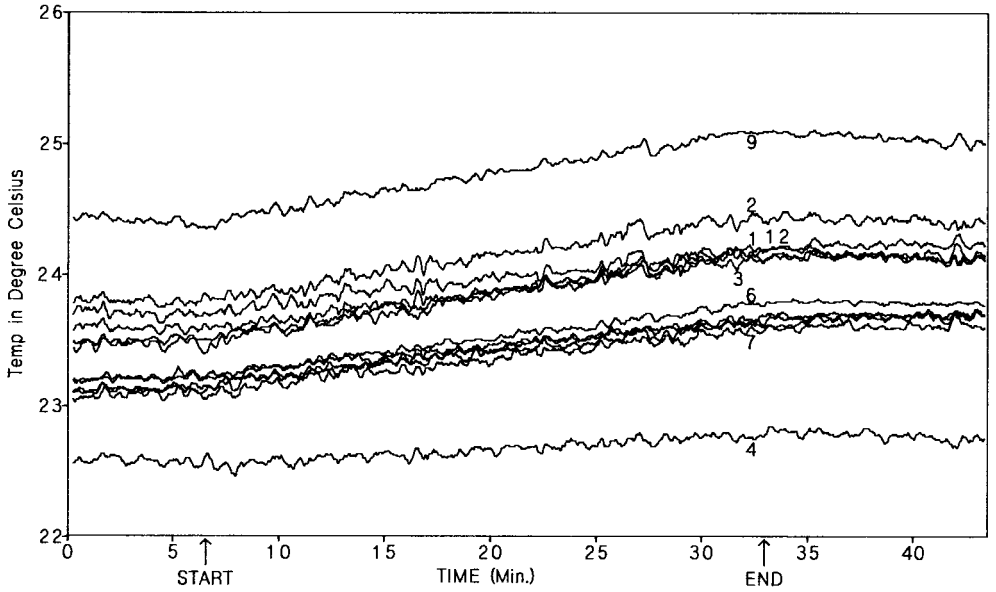

Fig. 7. Control temperature data during 26-min worst case MRI scan. Temperature sensors were at the same locations as shown in Fig. 2 without the SpF. Temperature elevations were less than 0.5 °C.

field enhancement due to external leads and implants in contact with tissues" had an analysis of the electric field at the tip of an insulated elongated metal implant. When a metal conductor (such as the lead) is exposed to an RF electromagnetic field, an RF current is induced in the conductor. The induced current is highest when the electric field is parallel to the conductor. The tangential electrical field is the same inside and outside of the conductor. For a very thin copper electrode implanted in muscle and exposed to 2450 MHz, the enhancement ratio can approach 8×10^6. Using thermograms, Johnson and Guy [18] showed that a standard coaxial electrode inserted in a cat brain for neurophysiological recordings increased specific absorption rate at the tip of the electrode by 50× (2.27 to 113 W/kg). In our study, RF current at the tip of the broken electrode caused excessive heating. When the implant was intact, the RF current emanated through the entire length of the bare electrode. No significant heating of the conductive electrode was observed. The insulation made the difference in heating. When only a very short conductor was in contact with tissue, significant heating occurred at the tip. In Fig. 4, the initial rate of temperature rise at Sensor #1 was 56.7 °C/min. Assuming no heat loss, the SAR at the tip of the broken wire was 3.4 kW/kg. This is three orders of magnitude higher that the whole-body averaged SAR of 1.095 W/kg. The equivalent induced electric field at the tip was 2060 V/m and the induced current 1650 A/m^2 (using the formulas in [2]).

It is noted in Figs. 4 and 5 that after the temperature rise reached 11–12 °C, it fluctuated. This was not observed in lower-temperature data. In the past, we have kept the maximum temperature rise in phantom muscle within 10 °C to

prevent a "thermal runaway" phenomenon. Why it fluctuates is not clear. Although the regular scan took only 4 min as compared to the 26-min worst scan, the maximum temperature rises were similar. This was not a surprise finding if whole-body SAR's were compared, i.e., 0.914 and 1.095 W/kg for the two scans, respectively. The thermal diffusion made the two cases saturate at similar temperatures. It was possible that the actual temperature rise was higher than measured. For the purpose of this study, exact temperature at that level was not essential. The major finding of this study was that it is unsafe to scan a patient wearing a spinal fusion stimulator with MRI if the stimulator lead is broken. According to the manufacturer, X-ray examination is the only simple way to find out whether the lead is broken.

V. Conclusion

The results show that for an SpF, when properly implanted, the maximum temperature rise in a static phantom model was less than 2 °C, which was within the FDA guidelines for the torso. However, if an electrode lead was broken, the temperature rise could be very high (14 °C). This exceeded the FDA regulation. Careful radiological examinations must be done to ensure that there are no broken leads in the patient before an MRI scan, although company records show that lead breakage is rare (10 broken leads in 50 000 patients). After the generator was removed, electrode heating was within the FDA guidelines. This study was done on a static phantom and, therefore, no blood flow was simulated. In a patient, due to blood flow, maximum temperature rise should be lower than the phantom model measurements. Therefore, this study provides a worst-case estimation.

Acknowledgment

The authors gratefully appreciate B. Simon of the Electro-Biology Inc. for providing all necessary support for this project. MRI scannings were performed on weekends by C. J. Torricelli, R.T., and K. L. Richau, R.T.

References

[1] FDA, "Recommendations and report on petitions for magnetic resonance reclassification and codification," Final Rule, 21 CFR Part 892. *Fed. Reg.*, vol. 54, no. 20, pp. 5077–5088, 1989.

[2] C. K. Chou, H. Bassen, J. Osepchuk, Q. Balzano, R. Petersen, M. Meltz, R. Cleveland, J. C. Lin, and L. Heynick, "Radio frequency electromagnetic exposure: A tutorial review on experimental dosimetry," *Bioelectromagn.*, vol. 17, no. 3, pp. 195–208, 1996.

[3] C. K. Chou, J. A. McDougall, and K. W. Chan, "Absence of heating from auditory implants during magnetic resonance imaging," *Bioelectromagn.*, vol. 16, no. 5, pp. 307–316, 1995.

[4] A. W. Guy and C. K. Chou, "Specific absorption rates of energy in man models exposed to cellular UHF-mobile-antenna fields," *IEEE Trans. Microwave Theory Tech.*, vol. MTT-34, no. 6, pp. 671–680, 1986.

[5] G. Hartsgrove, A. Kraszewski, and A. Surowiec, "Simulated biological materials for electromagnetic radiation absorption studies," *Bioelectromagn.*, vol. 8, no. 1, pp. 29–36, 1987.

[6] C. K. Chou, G. W. Chen, A. W. Guy, and K. H. Luk, "Formulas for preparing phantom muscle tissue at various radiofrequencies," *Bioelectromagn.*, vol. 5, no. 4, pp. 435–441, 1984.

[7] C. H. Durney, H. Massoudi, and M. F. Iskander, *Radiofrequency Radiation Dosimetry Handbook*, 4th ed. USAFSAM-TR-85-73, Brooks AFB, TX, 1986.

[8] K. A. Wickersheim and M. Sun, "Fiberoptic thermometry and its applications," *J. Microwave Power*, vol. 22, pp. 85–94, 1987.

[9] F. Shellock, D. Schaefer, W. Grundfest, and J. Crues, "Thermal effects of high-field (1.5 tesla) magnetic resonance imaging of the spine. Clinical experience above a specific absorption rate of 0.4 W/kg," *Acta. Radiol. Suppl.*, vol. 369, pp. 514–516, 1986.

[10] P. L. Davis, C. Shang, L. Talagala, and A. W. Pasculle, "Magnetic resonance imaging can cause focal heating in a nonuniform phantom," *IEEE Trans. Biomed. Eng.*, vol. 40, pp. 1324–1327, 1993.

[11] R. Buchli, P. Boesiger, and D. Meier, "Heating effects of metallic implants by MRI examinations," *Magn. Res. Med.*, vol. 7, pp. 255–261, 1988.

[12] J. X. Zhang, C. L. Wilson, M. F. Levesque, E. J. Behanke, and R. B. Lufkin, "Temperature changes in nickel-chromium intracranial depth electrodes during MR scanning," *Amer. J. Neuroradiol.*, vol. 14, pp. 497–500, 1993.

[13] L. L. Fagan, F. G. Shellock, R. J. Brenner, and B. Rothman, "*Ex vivo* evaluation of ferromagnetism, heating, and artifacts of breast tissue expanders exposed to a 1.5-T MR system," *J. Magn. Reson. Imag.*, vol. 5, pp. 614–616, 1995.

[14] F. G. Shellock, M. Nogueira, and S. M. Morisoli, "MR imaging and vascular access ports: *Ex vivo* evaluation of ferromagnetism, heating, and artifacts at 1.5 T," *J. Magn. Res. Imag.*, vol. 5, pp. 481–484, 1995.

[15] F. G. Shellock and S. M. Morisoli, "*Ex vivo* evaluation of ferromagnetism, heating, and artifacts produced by heart valve prostheses exposed to 1.5 T MR system," *J. Magn. Res. Imag.*, vol. 4, pp. 756–758, 1994.

[16] F. G. Shellock and E. Kanal, *Magnetic Resonance: Bioeffects, Safety, and Patient Management.* New York: Raven, 1994, p. 12.

[17] "Radiofrequency electromagnetic fields; properties, quantities and units, biophysical interaction, and measurements," Nat. Council Radiation Protection and Measurements, Bethesda, MD, NCRP Rep. 67, 1981.

[18] C. C. Johnson and A. W. Guy, "Nonionizing electromagnetic wave effects in biological materials and systems," *Proc. IEEE*, vol. 60, no. 2, pp. 692–718, 1972.

Chung-Kwang Chou (S'72–M'75–SM'86–F'89) was born in Chung-King, China, on May 11, 1947. He received the B.S. degree from National Taiwan University, Taipei, in 1968, the M.S. degree from Washington University, St. Louis, MO, in 1971, and the Ph.D. degree from the University of Washington, Seattle, in 1975, all in electrical engineering.

After spending a year as a National Institutes of Health Post-Doctoral Fellow in the Regional Primate Research Center and the Department of Physiology and Biophysics at the University of Washington, he served as Assistant Professor from 1977 to 1981 and Research Associate Professor from 1981 to 1985 at the Department of Rehabilitation Medicine and Center for Bioengineering of the University of Washington. In 1985, he moved to City of Hope National Medical Center, Duarte, CA, and is now the Director of the Department of Radiation Research. He has been engaged in teaching and research in electromagnetic dosimetry, exposure systems, and biological effects and medical applications of electromagnetic energy since 1971. His research at the City of Hope has been on hyperthermia for cancer treatment, electrochemical treatment of cancer, and RF dosimetry.

In 1981, Dr. Chou received the first special award for the decade (1970–1979) from the International Microwave Power Institute, in 1985, the outstanding paper award from the *Journal of Microwave Power*, and in 1995, the Curtis Carl Johnson Memorial Award for Preceptor of Best Student Poster from the Bioelectromagnetics Society. He was the Chairman of Microwave and RF Subcommittee (1990–1994) of the Committee on Man and Radiation, under the IEEE US Activities, and has served on the IEEE Scientific Coordinating Committee 28, Subcommittee 3 and 4, and as the Chairman of the Engineering Validation Group of SC4 since 1992. These committees are responsible for developing nonionizing radiation safety standards from dc to 300 GHz. He has served the Committee on Man and Radiation, now under EMBS, as Vice Chairman (1994–1995), and Chairman (1996–1997). Under the IEEE US Activities, he is a member of the Medical Technology Policy Committee (1995–). He was on the Board of Directors of the Bioelectromagnetics Society (1981–1984) and has been the Associate Editor of the *Journal of Bioelectromagnetics* since 1987, responsible for editing papers on high-frequency RF fields. He is a member of the Electromagnetics Academy (1990–) and a Distinguished Lecturer of IEEE Engineering in Medicine and Biology Society (1991–1992). In 1995, he was elected to serve as the Vice-Chairman of Committee 89-5 of the National Council on Radiation Protection and Measurements. He is a member of BEMS, AAAS, Radiation Research Society, North American Hyperthermia Society, Tau Beta Pi and Sigma Xi, and a Fellow of the American Institute for Medical and Biological Engineering.

John A. McDougall (M'87) received the B.A. degree in chemistry in 1953 and the B.S. degree in electrical engineering in 1965, both from the University of Washington, Seattle.

From 1953 to 1962, he served in the United States Air Force as a Squadron Officer and Pilot, and it was there that his interest changed from chemistry to electronics. In 1966, he became a Charter Member of what would become Bill Guy's Bioelectromagnetics Group at the University of Washington and remained there until 1985. During this period, he was instrumental in developing phantom modeling materials and thermographic techniques. In September 1985, he became a Senior Research Associate in the Department of Radiation Research of the City of Hope National Medical Center, Duarte, CA. His work there has included antenna development for intracavitary and interstitial hyperthermia, RF exposure systems, and dosimetry.

Kwok W. Chan (M'93) was born in Hong Kong, June 23, 1956. He received the B.S.E.E. degree in 1979 from the University of Nebraska, Lincoln, and the M.S.E.E. degree in 1982 from the University of Arizona, Tucson.

From 1982 to 1985, he worked at the University of Arizona Health Science Center engaging in hyperthermia research. In 1985, he joined the City of Hope National Medical Center, Duarte, CA, doing research on hyperthermia and electromagnetic dosimetry with experimental and numerical methods. His research interests include measurement techniques in high electromagnetic field environments and supercomputing for electromagnetic dosimetry.